Published by Avanti Publishers

International Journal of Petroleum Technology

ISSN (online): 2409-787X

Rock Typing and Characterization of the Late Cretaceous Abu Roash "G" Reservoirs at East Alam El-Shawish Field, Western Desert, Egypt

Marwan M. Sabry[1], Mohamed I. Abdel-Fattah[2,*] and Mohamed K. El-Shafie[3]

[1]*Petrosannan Petroleum Company, Cairo, Egypt*

[2]*Petroleum Geosciences & Remote Sensing Program, Department of Applied Physics and Astronomy, College of Sciences, University of Sharjah, Sharjah 27272, UAE*

[3]*Geology Department, Faculty of Science, Suez Canal University, Ismailia, Egypt*

ARTICLE INFO

Article Type: Research Article

Academic Editor: Adil Ozdemir

Keywords:
Abu Roash
Rock typing
Petrophysical analysis
Reservoir quality index
Reservoir characterization
Reservoir potentiality & flow zone

Timeline:
Received: August 26, 2023
Accepted: October 09, 2023
Published: November 01, 2023

Citation: Sabry MM, Abdel-Fattah MI, El-Shafie MK. Rock typing and characterization of the late cretaceous Abu Roash "G" reservoirs at East Alam El-Shawish field, Western Desert, Egypt. Int J Petrol Technol. 2023; 10: 115-134.

DOI: https://doi.org/10.15377/2409-787X.2023.10.9

ABSTRACT

Rock typing and petrophysical characterization play a vital role in constructing reservoir models for petroleum exploration and development. This study focuses on evaluating the petrophysical characteristics of the Late Cretaceous Abu Roash "G" Reservoirs at the East Alam El Shawish field in Egypt's Western Desert. The study involved five vertical wells and employed various techniques and analyses to investigate the reservoir. Lithology determination utilizing well logs and core analysis helps identify the lithology types and corresponding porosity of the Abu Roash "G" reservoirs. Sandstone and limestone lithologies with varying porosity ranges were identified, along with the influence of shale on neutron porosity values. Facies analysis of the Abu Roash "G" Member identified seven lithofacies types, categorized into shallow marine and deeper marine depositional environments. The petrophysical analysis involves evaluating gamma-ray logs, porosity, permeability, flow zone indicator (FZI), and reservoir quality index (RQI) values for each lithofacies type. This analysis classifies the core samples into seven reservoir rock types (RRT1 to RRT7) based on petrophysical attributes, providing a clear classification of the Abu Roash "G" reservoir interval. RRT1, RRT2, and RRT3 exhibit the highest reservoir quality, while RRT4 and RRT5 indicate moderate reservoir quality. RRT6 and RRT7 exhibit low reservoir quality due to unfavorable petrophysical behavior. The findings of this study provide valuable insights into the Abu Roash "G" reservoir, including its lithofacies, reservoir properties, and depositional environments. This knowledge is crucial for reservoir characterization and optimizing oil production strategies in the region.

*Corresponding Authors

Email: mfarag@sharjah.ac.ae
Tel: +(??) 13688465071

1. Introduction

Rock typing and petrophysical characterization are fundamental aspects of reservoir characterization and modeling in petroleum exploration and development [1, 2]. These processes play a crucial role in understanding the properties and behavior of reservoir rocks, which are essential for optimizing oil and gas production strategies [3-5]. Reservoir rock typing involves classifying reservoir rocks into distinct types based on their petrophysical and geological characteristics that influence fluid flow. It helps in identifying similarities and differences among rock samples, allowing for a better understanding of their behavior and performance within the reservoir [6]. The concept of reservoir rock typing has been widely recognized in the petroleum industry as a valuable tool for production and drilling operations [7].

One of the primary objectives of reservoir rock typing is to delineate specific regions within a reservoir, known as Hydraulic Flow Units (HFUs) [5, 8]. HFUs are regions characterized by similar hydraulic properties that control fluid flow within the reservoir. Understanding the distribution and properties of HFUs is essential for efficient reservoir management and production optimization [9]. By identifying different rock types and their associated HFUs, engineers can tailor their strategies and operations accordingly, focusing on areas with favorable properties for enhanced production.

Petrophysical characterization complements rock typing by providing quantitative measurements and analysis of the physical properties of reservoir rocks. It involves evaluating parameters such as porosity, permeability, saturation, and rock-fluid interactions [10, 11]. These measurements are crucial for determining the reservoir's ability to store and transmit hydrocarbons. Additionally, petrophysical characterization helps in estimating reserves, assessing reservoir quality, and predicting production performance.

Accurate rock typing and petrophysical characterization rely on various techniques and tools, including well logs, core analysis, laboratory measurements, and numerical modeling [12]. Well logs, acquired during the drilling process, provide valuable information about the subsurface formations, including lithology, porosity, and fluid content [13-15]. Core analysis involves extracting rock samples from the reservoir and subjecting them to laboratory tests to measure their physical properties. The importance of rock typing and petrophysical characterization in petroleum exploration and development cannot be overstated. Accurate reservoir characterization allows for a better understanding of the subsurface geology, identification of optimal drilling locations, estimation of reserves, and design of effective production strategies. It helps minimize risks, enhance production efficiency, and maximize economic returns.

This paper aims to explore the significance of rock typing and petrophysical characterization in reservoir studies, highlighting their importance and applications in the Late Cretaceous Abu Roash "G" Reservoirs at East Alam El-Shawish field, Western Desert, Egypt (Fig. **1**).

2. Geologic Setting

The northern Western Desert of Egypt is characterized by a litho-stratigraphic segment (Fig. **2**), with an overall thickness of 4270 meters [16, 17]. The Upper Cretaceous layers in the Abu Gharadig, Shushan, and Alamin basins of the Western Desert are known for their significant hydrocarbon exploration. Among these layers, the Upper Cretaceous "Abu Roash Formation" is particularly noteworthy as it signifies the onset of a substantial sea incursion in the study area, marked by the dominance of carbonate deposits [1, 18, 19]. Acting as a supportive layer for the Bahariya Formation, the Abu Roash Formation is divided into seven lithostratigraphic groups, labeled "G" to "A," representing the Upper Cenomanian to Santonian periods. The deposition of this formation occurred in multiple sedimentary cycles within a large, shallow marine environment [20, 21].

The Abu Roash Formation exhibits distinct cycles of sea-level oscillation, with clastic-dominated stages during regressive phases and limestone and shale deposition during transgressive phases [22]. El Gezeery *et al*. [23] further divided the Abu Roash Formation into seven groups: "G," "F," "E," "D," "C," "B," and "A." The thickness of this section generally increases northward in the northern Western Desert. The "A," "C," "E," and "G" members are predominantly composed of fine clastics, while the "B," "D," and "F" members consist of relatively clean carbonates [24-26].

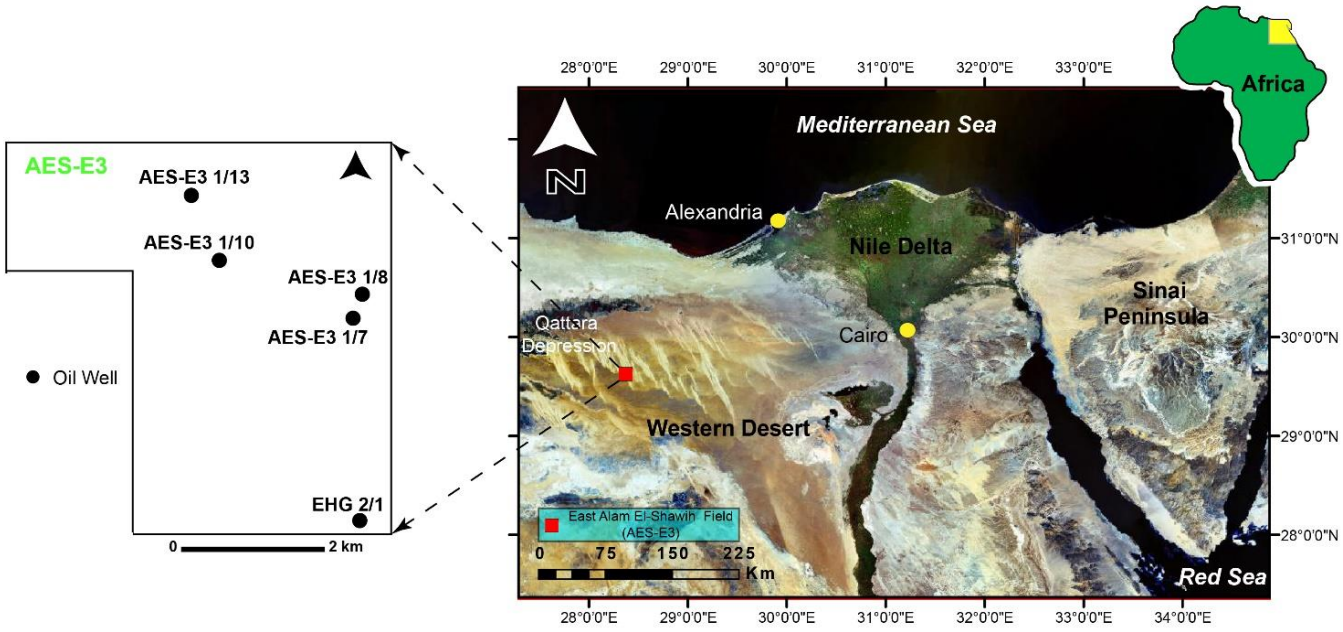

Figure 1: The location map of the study area in the East Alam El-Shawih (AES-E3) field, situated in the Western Desert of Egypt. The study area is highlighted in red color, indicating its boundaries within the Western Desert. Additionally, the locations of the studied wells are marked on the map.

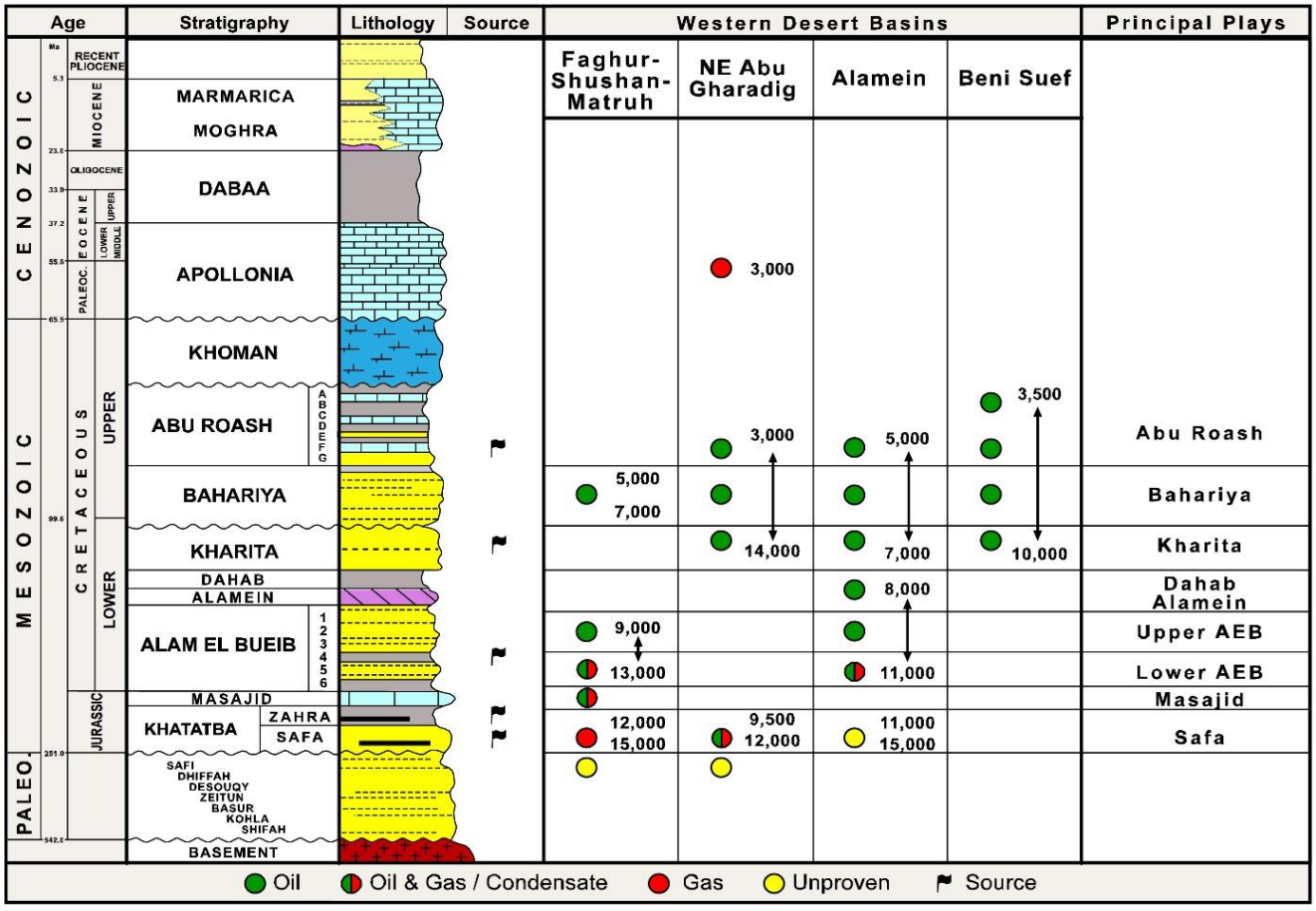

Figure 2: A generalized litho-stratigraphic column of the northern Western Desert of Egypt (Abdel-Fattah *et al*., 2018). The litho-stratigraphic column provides a vertical representation of the various rock units present in the region, depicting their relative positions and relationships.

Within the Abu Roash Formation, the Abu Roash "G" Member is a significant reservoir for oil production in the Razzak and Alamein fields [22]. It primarily comprises limestone interbedded with shale and dolomite layers. Additionally, the Abu Roash "G" Member holds potential as a source rock due to its high total organic content (TOC). It has been identified as a source rock in the Gindi basin [27, 28]. Studies have also highlighted the impact of diagenesis on the reservoir quality evolution of the late Cenomanian Abu Roash "G" Member in the Sitra field, North Western Desert, Egypt, and its potential as a reservoir and source rock in the Abu Gharadig basin, characterized by marginal/shallow marine environments [29]. In the Qarun and West Qarun area, the Abu Roash "G" Member is considered a source rock [27], and in the South Matruh area, it is recognized as a potential source rock.

The Late Cretaceous Abu Roash "G" formation in the Western Desert of Egypt has a rich sedimentary history that provides valuable insights into the geological past of the region [30]. During the Late Cretaceous period, approximately 100 to 66 million years ago, Egypt's Western Desert was submerged by a vast epicontinental sea known as the Tethys Ocean. The Abu Roash "G" formation was deposited during this time, reflecting a dynamic interplay of marine and terrestrial environments. This formation represents a critical chapter in the geological history of the area, recording the ebb and flow of ancient seas and the shifting patterns of sedimentation [31].

The facies description of the Abu Roash "G" formation reveals a diverse array of sedimentary environments. In marine settings, marine shales dominate, characterized by fine-grained sediments rich in organic matter [32, 33]. These shales point to periods of relatively calm marine conditions and are often considered source rocks for hydrocarbons. Additionally, marine limestones may be present, indicating times of carbonate deposition during rising sea levels. Marine sandstones, coarser in grain size, hint at nearshore or deltaic settings where sediment was transported by rivers and currents [34]. Terrestrial facies are also notable, featuring fluvial and deltaic deposits with sandstones and conglomerates, reflecting high-energy environments associated with river and delta activity. Interbedded shales within these facies suggest variations in sediment input and water energy levels [35, 36].

The transitional facies found in the Abu Roash "G" formation provide further evidence of the ever-shifting Late Cretaceous shoreline, highlighting the dynamic nature of sedimentary deposition in the region [37, 38]. Overall, this formation's sedimentary history and facies diversity offer valuable information for geological studies and hydrocarbon exploration, as they help geologists unravel the ancient environmental conditions and identify potential reservoirs and source rocks within this geological formation.

3. Materials and Methods

In the study conducted in the East Alam El-Shawish Area of the Western Desert in Egypt, five wells were analyzed to assess the petrophysical characteristics of the Abu Roash "G" reservoir. The wells included EHG 1/1, EHG 2/1, AES-E3 1-8, AES-E3 1-10, and AES-E3 1-13. A comprehensive set of well logs, such as density, gamma ray, neutron, sonic, PEF, and resistivity logs, along with core samples, were utilized for the analysis. The main objective was to calculate important reservoir parameters such as shale volume, porosity, and water saturation. This petrophysical analysis using well logs is a well-established method for estimating water, gas, and oil volumes in a specific formation [39, 40].

To perform the formation evaluation, the collected data underwent careful editing and correction. The formation evaluation aimed to calculate various parameters related to the reservoir, including thickness (total, net sand, net pay), total and effective porosity, volume of shale, and water and hydrocarbon saturation for the Upper Cretaceous Abu Roash "G" Reservoirs in the East Alam El-Shawish Area of the Western Desert, Egypt.

Different methods were employed to determine lithology from the good logs using various cross-plots. These cross-plot integration techniques were based on previous works by [41, 42]. Cross plots of two and three logs of porosity were utilized to display both lithology and porosity information. Specifically, the study utilized the Natural Gamma Ray Spectrometry (NGS) cross plot, neutron-density cross plot, and M-N cross plot. M-N diagrams were employed to facilitate the interpretation of rocks based on neutron, density, and sonic logs. This chart, initially

published by [43], utilizes three porosity logs to define the lithology-dependent quantities, M and N, which are independent of primary porosity. The M-N plot provides a clearer visualization of the lithological features. M and N are defined using specific equations that involve various log readings and density values. By plotting the organized values of M against N, minerals can be identified based on their position on the M-N plot.

Porosity, a crucial parameter for reservoir characterization, was determined using sonic, density, neutron, and core measurements. The gamma-ray log was used to calculate the shale volume (VSH) in each reservoir interval. The Techlog Petrophysics software played a crucial role in evaluating and interpreting the well-log data. Additionally, core samples were obtained from the AES-E3 1-10 well, specifically from the Abu Roash "G" reservoir, and EPRI Services (Egypt) conducted normal core analyses on these samples. The core analyses included measurements of grain density, permeability (vertical and horizontal), and porosity (helium and fluid summation). Approximately 110 samples were taken from a depth range of 3075 to 3084 meters in the AES-E3 1-10 well.

Reservoir rock typing, which involves accurately describing a reservoir's fluid movement capacity (permeability) and storage capacity (porosity), is a challenging task. This is accomplished by using a combination of core, well-log, and regular core analysis (RCAL) data. Another significant challenge is the identification of various rock types within a hydrocarbon resource. The concept of "electrofacies," introduced by [39], has become a valuable approach to differentiate different rock types using log responses. Electrofacies can be identified through manual examination of log patterns or by utilizing cluster analysis techniques [5, 44].

Facies analysis involves grouping certain properties of rocks, such as mineralogy, texture, fossils, and depositional environment, under the general name "facies." The term "facies" is commonly used to describe carbonate rocks and is also known as "microfacies" when discussing clastic rocks like sandstone. Facies associations, which are collections of related sedimentary facies, are used to describe specific geological environments. A sedimentary or depositional environment encompasses different processes involved in the deposition of a particular kind of sediment and the types of rocks that form through lithification and preservation over geological time.

Hydraulic flow units (HFUs) are correlative and mappable zones within a reservoir that regulate fluid flow [6]. Understanding fluid flow behavior is crucial, and flow zone indicators (FZIs) define each hydraulic flow unit and play a significant role in this understanding [17, 45]. The relationship between FZI, reservoir quality index (RQI), and void ratio (Z) can be described using equations. Plotting porosity (φ) against permeability (K) on a semi-log plot allows for clustering samples with similar FZI values, providing a better understanding of permeability variations within a reservoir. Techniques described in the literature are utilized to categorize log FZI data and determine hydraulic flow units.

4. Results

4.1. Lithology Determination of the Abu Roash "G"

The lithology determination of the Abu Roash "G" reservoir relied on the utilization of neutron-density cross plots and M-N cross plots (Fig. **3**-**4**). These techniques provided valuable insights into the composition and characteristics of the reservoir's lithologies, particularly focusing on sandstone and limestone, while also considering the influence of shale on neutron porosity values.

Neutron-density cross plots are widely employed in geology to accurately assess matrix porosity in carbonate rocks. By plotting bulk density (RHOB) and neutron porosity (NPHI) measurements together, specific lithologies saturated with water, such as sandstone, limestone, and dolomite, can be identified. These lithology lines represent varying degrees of porosity, offering crucial information about the rock's properties. In cases where lithologies exhibit binary complexity, like sand-lime or lime-dolomite, the plotted points derived from log measurements fall within the respective lithology lines. This allows for precise lithology determination based on the cross-plot analysis. The analysis of the cross plot for the Abu Roash "G" reservoir revealed significant findings (Fig. **3**). Points on the plot representing sandstone were observed, indicating the presence of this lithology within the reservoir. Additionally, there were points clustered around limestone, specifically calcareous sandstone, which

further contributed to the understanding of lithological composition. The presence of these lithologies was determined through the positioning of the plotted points relative to the lithology lines on the cross plot.

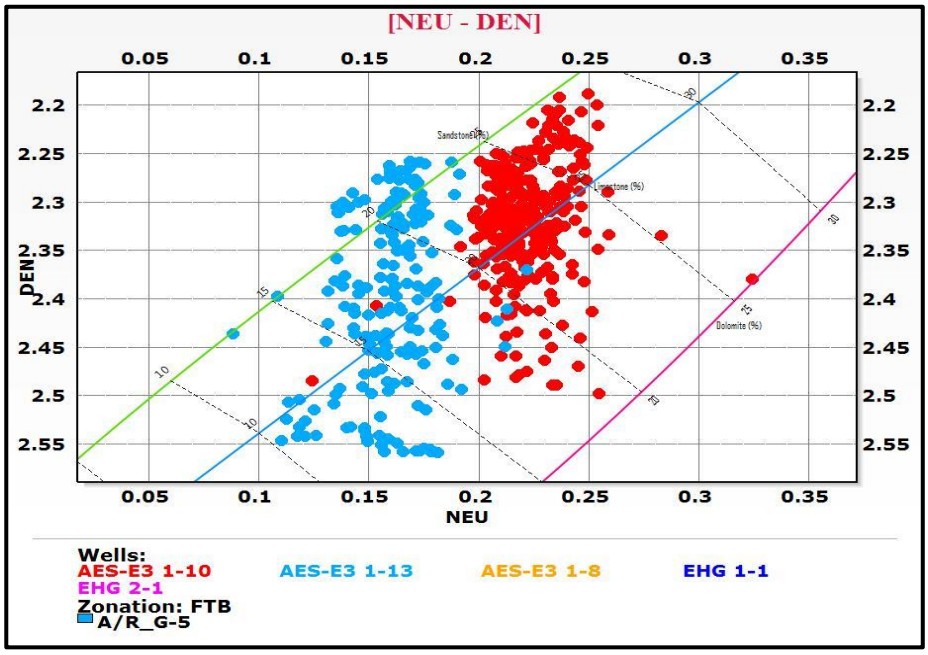

Figure 3: A Neutron-Density cross plot illustrates the lithology composition of the Abu Roash 'G' Reservoir.

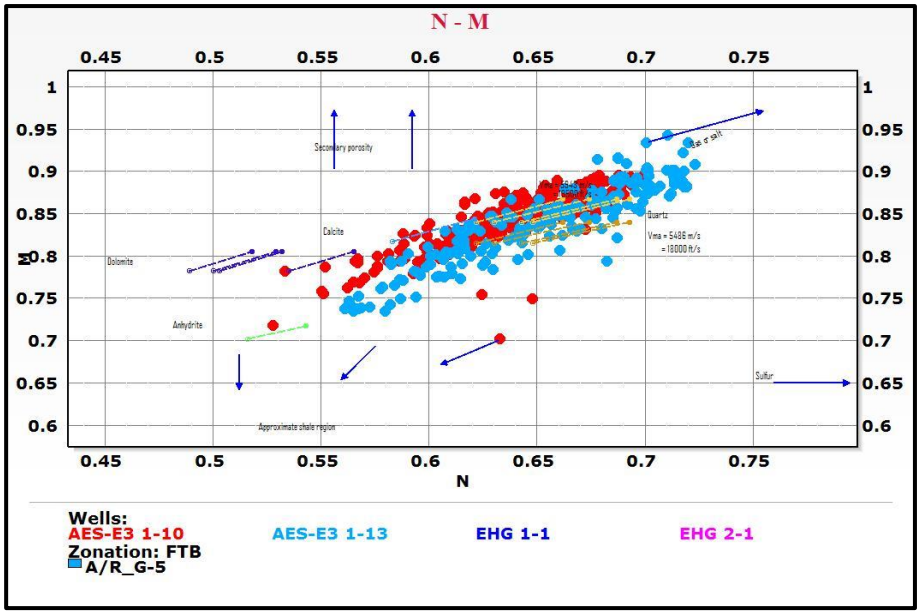

Figure 4: A M-N cross plot illustrates the lithology composition of the Abu Roash 'G' Reservoir.

Furthermore, the cross-plot analysis identified the gas effect and shale effect. The gas effect manifests as a shift in the plotted data towards the northwest from the sandstone line (Fig. **3**). This shift occurs when the presence of gas decreases neutron porosity and increases porosity calculated from density measurements. By examining the cross plot, geologists can gain insights into the impact of gas on the reservoir's characteristics. The shale effect, on the other hand, is observed when the effect of shale appears within the cross plot, tending towards the southeast. This effect, as described by [41], helps us understand the influence of shale on the reservoir. The identification of the shale effect aids in accurately assessing lithology and porosity, providing a more comprehensive understanding of the reservoir's composition. The average porosity within the Abu Roash "G"

reservoir was found to range from 12% to 26%. This variation in porosity values underscores the heterogeneity of the lithologies present and highlights the significance of porosity assessment in characterizing the reservoir.

Additionally, the M-N cross-plot analysis was employed to enhance the lithology determination of the Abu Roash "G" reservoir (Fig. **4**). By examining the cross-plot specifically generated using neutron porosity (NPHI) and micro-resistivity (M) measurements, further insights into lithology were obtained. The results of the M-N cross-plot analysis aligned with those from the neutron-density cross-plot, with points representing sandstone lithology observed. Furthermore, points around calcite, specifically calcareous sandstone, were identified, confirming the lithological composition of the reservoir. It is important to note that the presence of shale had a noticeable influence on the neutron porosity values, as seen in both the neutron-density cross-plot and the M-N cross-plot analyses. The shale effect was observed in the southeast direction, indicating the impact of shale on the reservoir's characteristics.

4.2. Facies Analysis of the Abu Roash "G"

The cored intervals of the Abu Roash "G" Member in the AES-E3 (1-10) will exhibit a vertical sequence of lithologies characterized by various colors and sedimentary features (Fig. **5**). The lithological variations noted comprise pale white, whitish grey, brownish grey, and brown vuggy textures, featuring phosphatic, argillaceous, dolomitic, bioturbated, glauconitic, and carbonaceous components. Additionally, there are segments of hard to very hard limestone, along with intercalated layers of grey, hard to medium-hard marl. Fig. (**3**) offers a graphical depiction of these diverse lithological characteristics.

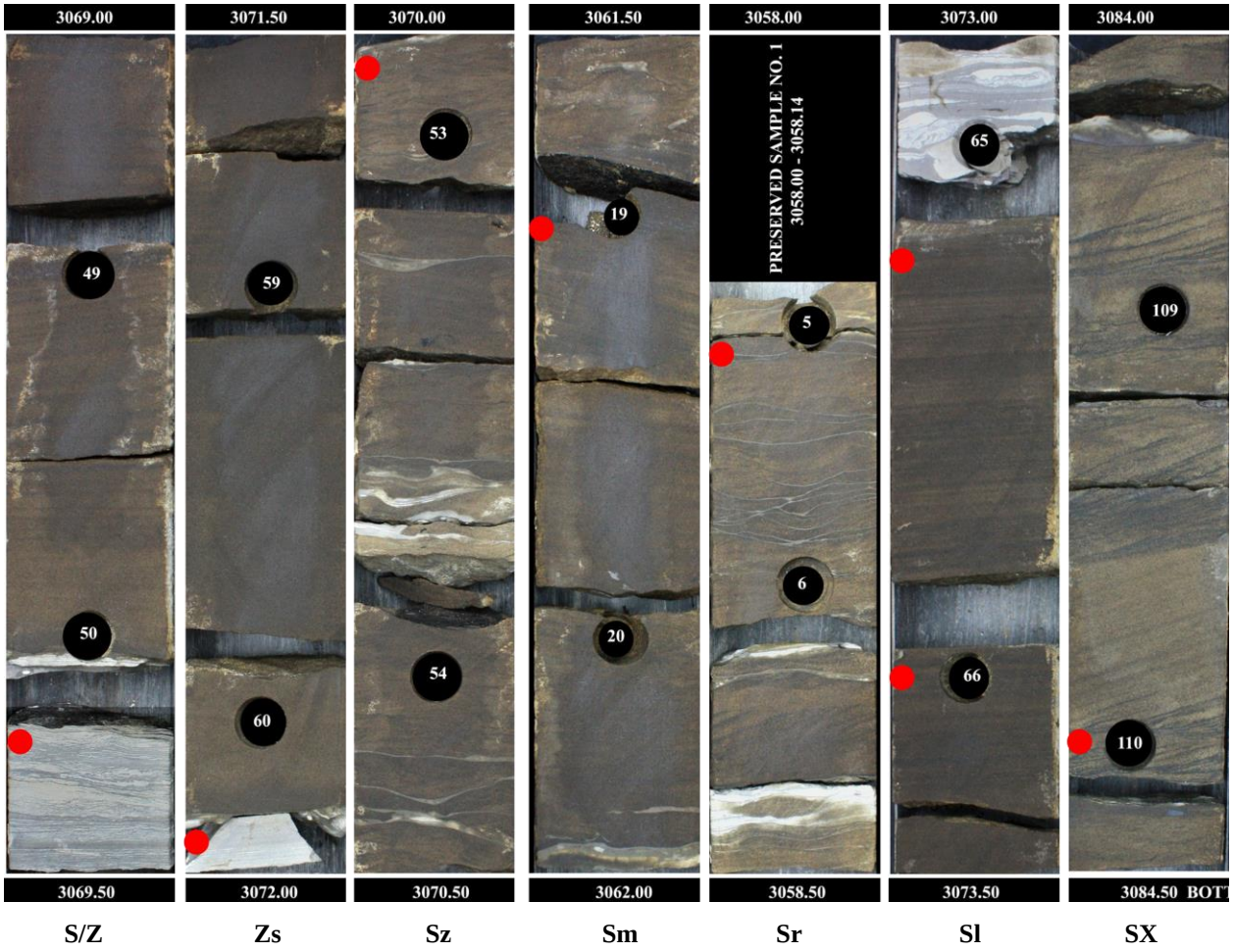

Figure 5: Core samples from the Abu Roash "G" reservoir at the East Alam El-Shawish field in the Western Desert of Egypt. The core samples reveal the presence of seven distinct reservoir rock types (RRT) within the reservoir.

Within this lithological sequence, there are sandstone facies that exhibit different characteristics. The sandstone facies exhibit a range from hard to moderately hard textures and are reasonably well-sorted, composed of fine to very fine sand grains. They display colors such as grey, yellowish, brownish-gray, light brown, and greenish-gray, particularly in highly glauconitic levels. These sandstones possess varying degrees of silt, clay, calcareous material, and bioturbation. Some intervals show a mottled appearance with preserved wavy argillaceous laminations, while others appear massive or ripple laminated. Carbonaceous matter can be locally present in certain parts of the sandstone facies. Other minerals identified include pyrite, opaque minerals, iron oxides, and phosphate. Grey to dark grey shale, silty shale, and sandy shale are also observed within the lithological sequence.

Based on a detailed sedimentary facies analysis, seven distinct lithofacies types have been identified within the cored intervals. These lithofacies can be grouped into two facies associations, which represent assemblages of related lithofacies. Table **1** provides an overview of the identified facies codes. The characteristics of these facies associations, including lithology, color, primary sedimentary structures, vertical distribution, and probable depositional environments, are described further.

Table 1: A summary of the lithofacies and petrophysical characteristics of the ARG reservoir, based on measurements from the core and electrical logs.

RRT	Lithofacies	Porosity (%)	Permeability (mD)	Grain Density	PHIZ	RQI	FZI
RRT1	Cross Bedded Sandstone	24-26	>1000	2.31-2.39	0.31-0.33	1.7-2.25	6.5-8
RRT2	Laminated Sandstone	17-25	300-700	2.3-2.39	0.21-0.32	1.3-1.7	5.3-6.5
RRT3	Rippled Sandstone	14-25	300-600	2.28-2.39	0.16-0.32	1.15-1.6	4.5-5.3
RRT4	Massive Sandstone	16-27	200-400	2.24-2.43	0.19-0.36	0.95-1.35	3.5-4.5
RRT5	Silty Sandstone	12-27	50-250	2.2-2.42	0.12-0.34	0.38-1.15	2.5-3.5
RRT6	Heterolithic alternated sandstone and thin layers silt	15-24	10-100	2.22-2.36	0.18-0.3	0.31-0.7	1.7-2.5
RRT7	Sandy Siltstone	5-15	0.01-10	2.33-2.48	0.02-0.22	0.05-0.36	0.5-1.7

The first facies association comprises lithofacies types characterized by pale white to whitish grey limestone with vuggy, phosphatic, and argillaceous components. These lithofacies exhibit vertical variations and are interpreted to have been deposited in a shallow marine environment. The second facies association includes lithofacies types consisting of glauconitic, phosphatic, carbonaceous matter-bearing, hard to very hard limestone, along with interbeds of marls. These lithofacies are believed to have been deposited in a relatively deeper marine environment. Additionally, the facies associations provide insights into the potential reservoir quality of these lithologies.

4.2.1. Heterolithic Sand / Silt Argillaceous Siltstone: (S / Z Zs)

The facies association depicted in Fig. (**5**) consists of grey to brownish-grey sand/silt heterolithics and sandy siltstones. These lithologies exhibit a hard consistency. Within this facies association, various features and minerals have been identified, including carbonaceous matter, pyrite, opaque minerals, and mica.

The sedimentological parameters associated with this facies group suggest a most probable depositional environment of a mixed tidal flat. The presence of sand and silt heterolithics, along with sandy siltstones, indicates a combination of coarser and finer sediment grains. The hardness of the lithologies suggests some degree of compaction or cementation. The occurrence of carbonaceous matter, pyrite, opaque minerals, and mica may indicate organic-rich sediments and the influence of diagenetic processes.

Based on these sedimentological characteristics, it is inferred that this facies association was deposited in a mixed tidal flat environment. Tidal flats are transitional zones between terrestrial and marine environments,

influenced by tidal currents and characterized by fluctuating water levels. The mixture of sand and silt suggests a dynamic sedimentary setting with varying energy levels. The presence of carbonaceous matter and other minerals further supports the interpretation of organic-rich sediments, which can be associated with stagnant or brackish water conditions typical of tidal flat environments.

4.2.2. Silty, Massive, Ripple, Laminated, and Cross Bedded Sandstone: (Sz-Sm-Sr-Sl-Sx)

The sandstone within this facies group, as shown in Fig. (**5**), exhibits a range of colors from brownish grey to light brown to dark brown. It displays variable lithological characteristics, including parts that are argillaceous and slightly calcareous. Bioturbation is observed in certain intervals, indicating the activity of burrowing organisms within the sediment.

Within this facies group, sedimentary structures such as flaser and ripple laminations are present in localized intervals. Some intervals exhibit a massive structure, while others display cross-bedding and lamination. Additionally, the presence of carbonaceous matter and mica is observed in certain intervals. Pyrite and opaque minerals are recorded in parts of the sandstone. The sediment is silty, argillaceous, calcareous, and bioturbated in some sections.

The combination of these sedimentological features strongly suggests a depositional environment of a shallow marine tidal sand flat. The variable colors, presence of flaser and ripple laminations, bioturbation, and the characteristics of the sediment all indicate the influence of tidal currents and the dynamic nature of a shallow marine setting. The presence of carbonaceous matter and mica may suggest organic-rich conditions within the sediment, potentially contributing to its reservoir potential.

Based on the sedimentological analysis, this facies association within the sandstone with its specific lithological characteristics and sedimentary structures is considered to have the best reservoir potential. The observed features indicate the deposition in a shallow marine tidal sand flat environment, which is known for its favorable conditions for hydrocarbon reservoir development.

4.3. Rock Typing and Petrophysical Analysis of the Abu Roash "G"

The objective of this study is to analyze and predict the petrophysical behavior, reservoir characteristics, and the influence of common petrophysical attributes on core samples from the Abu Roash "G" sand reservoir. The core samples were thoroughly assessed and classified into seven reservoir rock types, labeled as RRT to RRT7, based on a comprehensive petrophysical assessment and core description, as depicted in Fig. (**6**).

The gamma-ray logs obtained from the Abu Roash G-5 reservoir reveal distinct patterns characterized by boxcar (or blocky), serrated, and cylindrical themes, as shown in Fig. (**4**). The gamma-ray levels of this facies range from 30 to 150 API units, with an average thickness of 25 meters. Based on the well-log analysis, the primary lithology identified in this facies is sandstone with varying amounts of silt and shale. Additionally, the grain size variation observed in the log character from the base to the top reflects a fining upward trend.

Among the categorized reservoir rock types, RRT1 samples correspond to Cross Bedded Sandstone, exhibiting an average grain density ranging from 2.31 to 2.39 g/cm3. These samples display exceptional reservoir attributes, characterized by remarkably high porosity levels ranging from 24% to 26% and very good permeability values in the range of 1000 millidarcies (mD). The average flow zone indicator (FZI) values indicate a very good reservoir quality, ranging from 6.5 to 8 meters, while the average reservoir quality index (RQI) values suggest a very good reservoir quality ranging from 1.7 to -2.25 meters.

Laminated sandstone samples, classified as RRT2, exhibit an average grain density between 2.3 and 2.39 g/cm3. These samples demonstrate very good porosity levels ranging from 17% to 25% and extremely good permeability values ranging from 300 to 700 mD. The average FZI values of this rock type indicate a very good reservoir quality, ranging from 5.3 to 6.5 meters, while the average RQI values also suggest a very good reservoir quality, ranging from 1.3 to -1.7 meters (Fig. **7**).

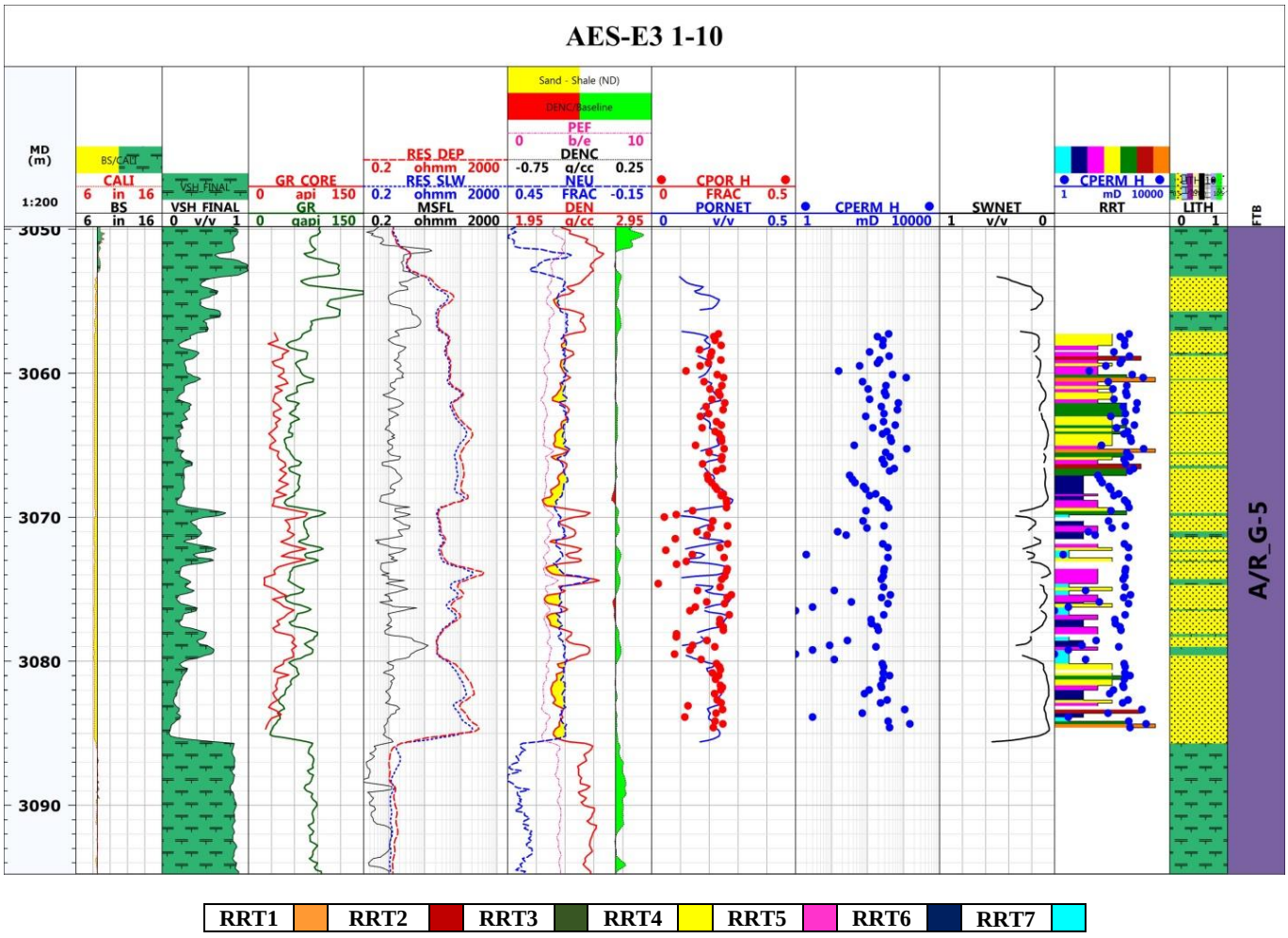

Figure 6: The seven reservoir rock types (RRT) encountered in the Abu Roash "G" formation, specifically from the AES-E3 1-10 well at the East Alam El-Shawish field in the Western Desert of Egypt. The figure also displays the gamma ray logs motifs, highlighting the fining upward character observed from the base to the top of the Abu Roash G-5 reservoir in the AES-E3 1-10 well. The comparison between open-hole log results and core data reveals a robust 96% correlation in calculated porosity. Furthermore, variations in porosity and permeability indicate differing reservoir quality levels, with RRT1 (indicative of good quality) positively linked to high porosity and permeability, while RRT7 (representing lower quality) exhibits an opposite relationship.

The petrophysical analysis of the RRT3 samples reveals that they are Rippled Sandstone, with an average grain density ranging from 2.28 to 2.39 g/cm3. These samples exhibit extremely good permeability values ranging from 300 to 600 mD and very good porosity levels ranging from 14% to 25%. The average RQI values for this rock type range from 1.15 to -1.6 meters, indicating a very good reservoir quality, while the average FZI values range from 4.5 to 5.3 meters, also indicating a very good reservoir quality (Fig. **8**).

Samples categorized as RRT4 represent Massive Sandstone, with an average grain density ranging from 2.24 to 2.43 g/cm^3. These samples exhibit good porosity levels ranging from 16% to 27% and good permeability values ranging from 200 to 400 mD. The average FZI values indicate a moderate reservoir quality, ranging from 3.5 to 4.5 meters, while the average RQI values range from 0.95 to -1.35 meters, respectively.

The Silty Sandstone samples, identified as RRT5, exhibit an average grain density ranging from 2.2 to 2.42 g/cm^3. These samples display good porosity levels ranging from 12% to 27% and moderate permeability values ranging from 50 to 250 mD. The average FZI values indicate an intermediate reservoir quality, ranging from 2.5 to 3.5 meters, while the average RQI values range from 0.38 to 1.15 meters, suggesting a moderate reservoir quality (Fig. **9**).

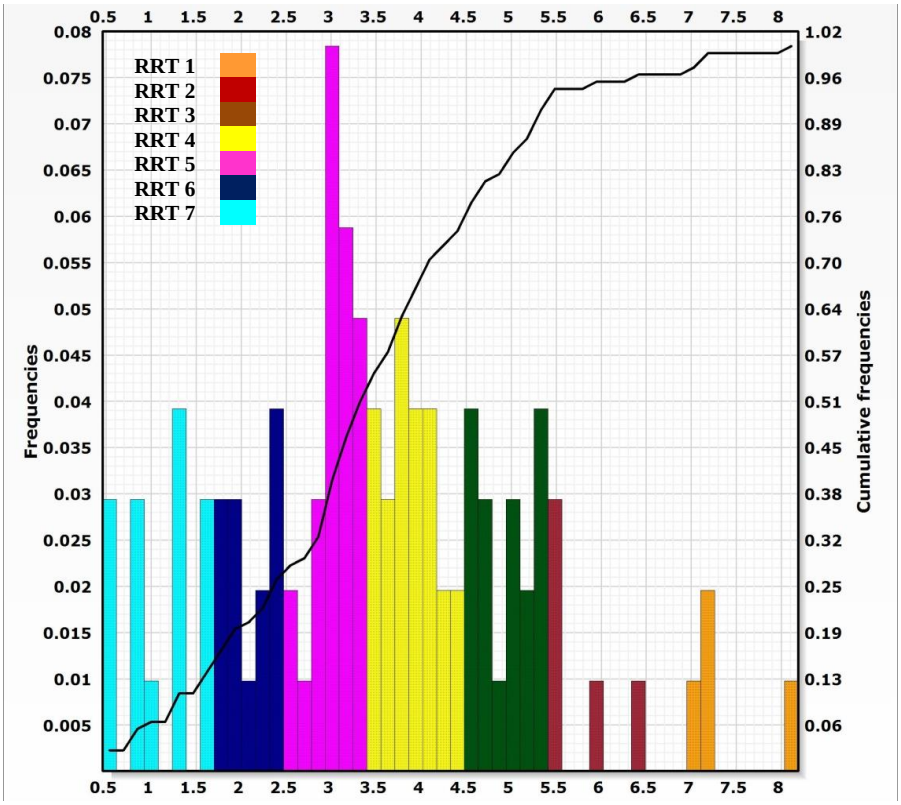

Figure 7: The Flow Zone Indicator (FZI) range of the different rock types (RRT1 to RRT7) within the Abu Roash "G" interval, specifically derived from the AES-E3 1-10 well at the East Alam El-Shawish field in the Western Desert of Egypt.

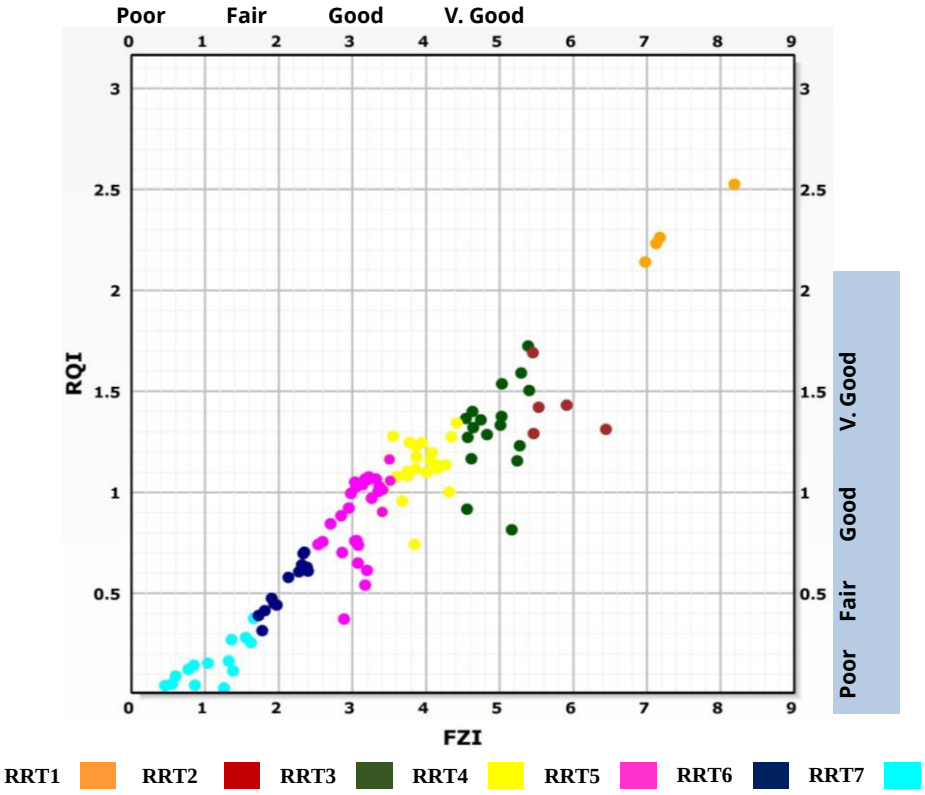

Figure 8: The relationship between the Flow Zone Indicator (FZI) and the Reservoir Quality Index (RQI) within the Abu Roash "G" reservoir interval, specifically derived from the AES-E3 1-10 well at the East Alam El-Shawish field in the Western Desert of Egypt.

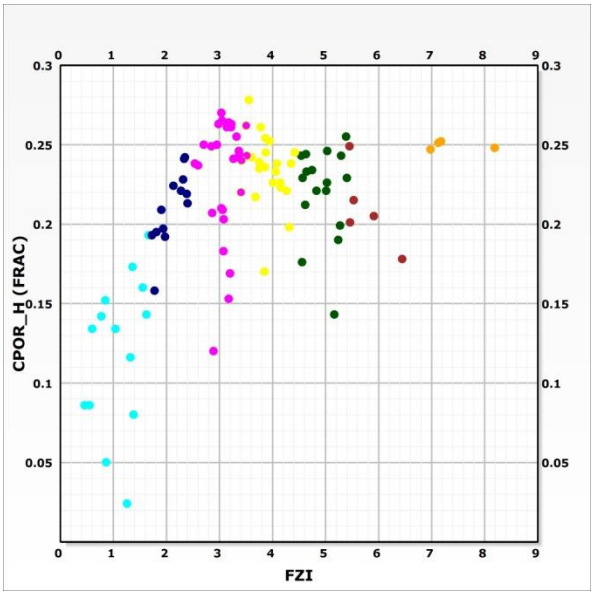

FZI VS Core Porosity

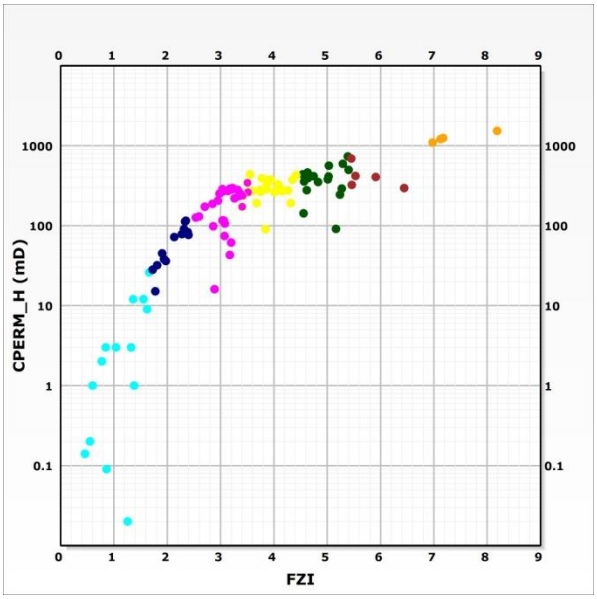

FZI VS Core Permeability

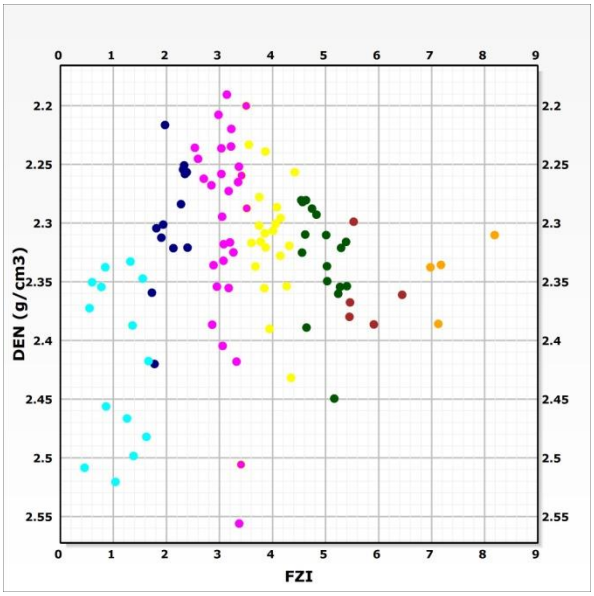

FZI VS Grain Density

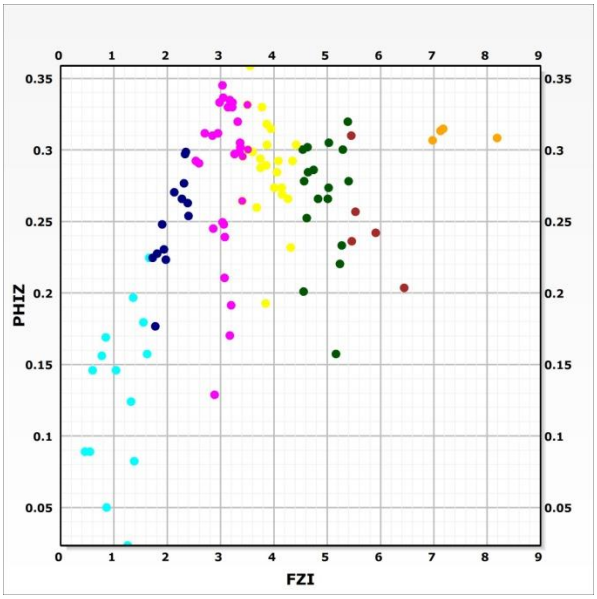

FZI VS PHIZ

RRT1 RRT2 RRT3 RRT4 RRT5 RRT6 RRT7

Figure 9: The Flow Zone Indicator (FZI) analysis of the Abu Roash "G" reservoir interval derived from the AES-E3 1-10 well at the East Alam El-Shawish field in the Western Desert of Egypt.

RRT6 samples represent Heterolithic Alternating Sandstone, characterized by alternating sandstone and thin silt layers, with an average grain density ranging from 2.22 to 2.36 g/cm^3. These samples exhibit low porosity levels ranging from 15% to 24% and low permeability values ranging from 10 to 100 mD. The average FZI values suggest a low reservoir quality, ranging from 1.7 to 2.5 meters, while the average RQI values range from 0.31 to 0.7 meters, indicating a low reservoir quality.

Finally, RRT7 samples represent Sandy Siltstone, exhibiting an average grain density ranging from 2.33 to 2.48 g/cm^3. These samples display low porosity levels ranging from 5% to 15% and very low permeability values ranging from 0.01 to 10 mD. The average FZI values indicate a very poor reservoir quality, ranging from 0.5 to 1.7 meters, while the average RQI values range from 0.05 to 0.36 meters, suggesting a low reservoir quality (Fig. **8**).

Fig. (**10**) illustrates the well log correlation among wells EHG 2-1, EHG 1-1, AES-E3 1-8, AES-E3 1-10, and AES-E3 1-13, highlighting the structural variations and facies changes within the Abu Roash "G" reservoir. This figure provides insights into the spatial distribution of different lithologies and their variations across the wells, offering valuable information about the reservoir's structural complexity and facies heterogeneity.

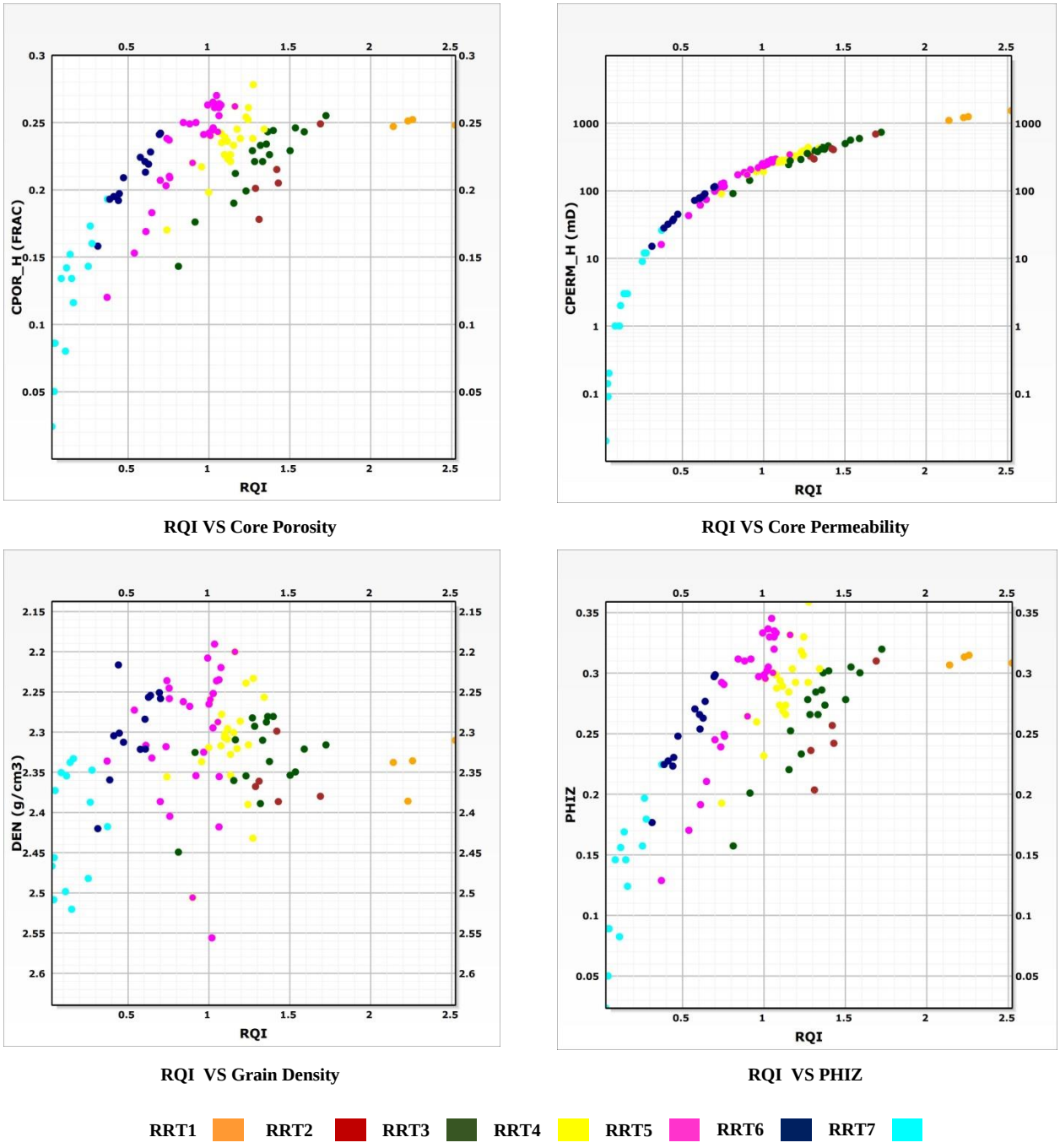

Figure 10: The Reservoir Quality Index (RQI) analysis of the Abu Roash "G" reservoir interval obtained from the AES-E3 1-10 well at the East Alam El-Shawish field in the Western Desert of Egypt.

Well-log correlation among multiple wells provided insights into the spatial distribution of lithologies and their variations, revealing the reservoir's structural complexity and facies heterogeneity. The analysis highlighted the predominance of sandstone zones within the reservoir and emphasized the significance of targeting these zones for production (Fig. **11**).

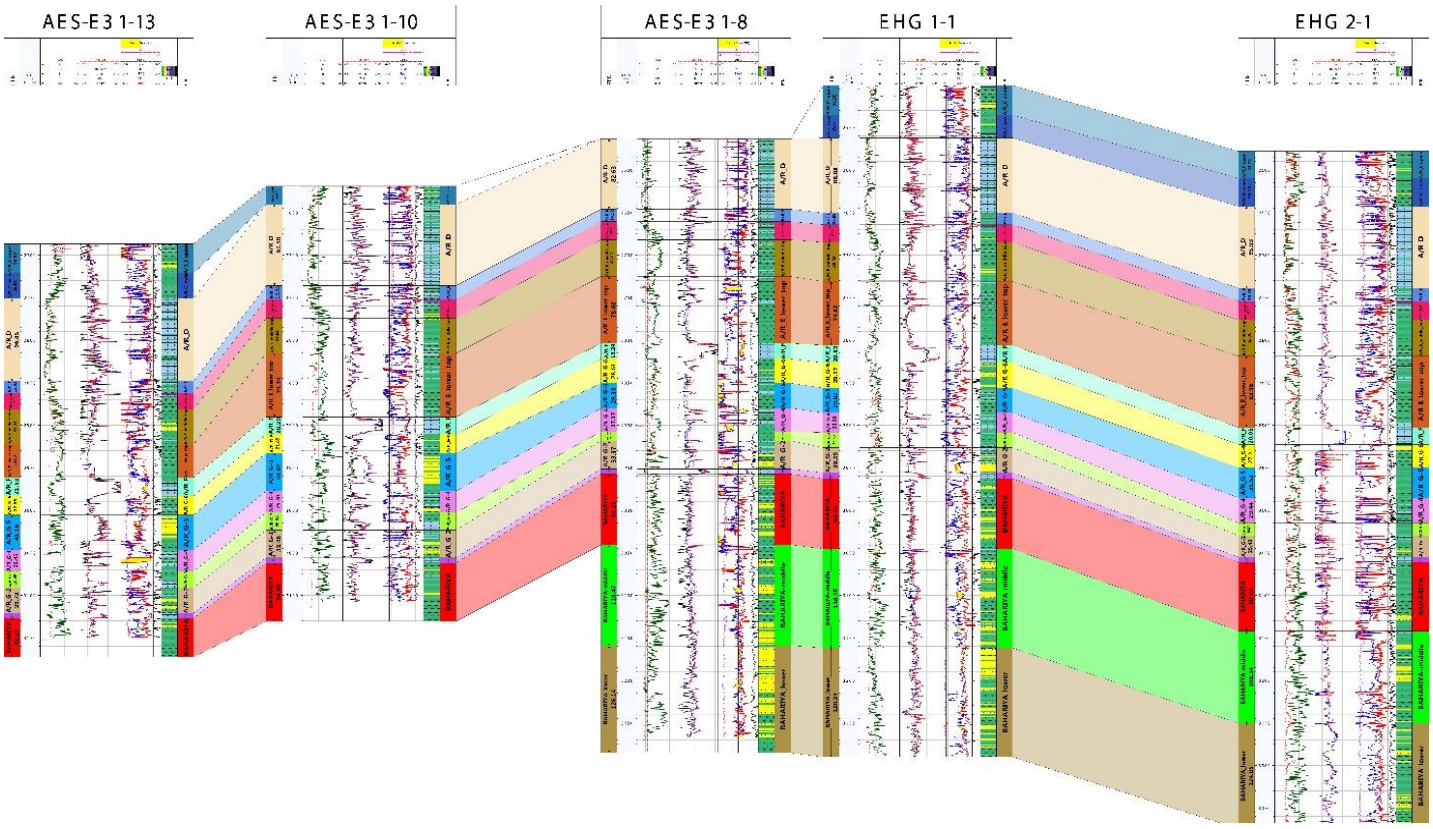

Figure 11: The well log correlation among wells EHG 2-1, EHG 1-1, AES-E3 1-8, AES-E3 1-10, and AES-E3 1-13, showcasing the structural variations and facies changes within the Abu Roash "G" reservoir.

The analysis of the Abu Roash "G" reservoir in the EHG 1-1 well (Fig. **11**) reveals that the reservoir is predominantly composed of shale intercalated with thin layers of limestone, with no presence of sand. Consequently, the production from this reservoir is expected to come from the sandstone zones within the formation. Similarly, the analysis of the Abu Roash "G" reservoir in the EHG 2-1 well (Fig. **12**) shows that it primarily consists of shale and limestone, with no sand. Therefore, the expected production is also from the sandstone zones in the formation. In the AES-E1 1-8 well, the Abu Roash "G" reservoir exhibits an intercalation of shale and thin layers of limestone, without any sand content. Hence, the production anticipated from the sandstone zones in the formation (Fig. **11**-**12**) demonstrates the vertical analysis of the Abu Roash "G-5" reservoir in the AES-E1 1-10 well. This reservoir is composed of shale with intermittent layers of sandstone and thin limestone layers. The fluid analysis indicates the presence of a gross sand thickness of 25.6 meters, with a net pay thickness. Additionally, the hydrocarbon saturation is observed to increase up to 90%. As a result, the production is expected from the sandstone zones within this reservoir. The analysis of the Abu Roash "G" reservoir in various wells consistently reveals the dominant lithology of shale intercalated with thin layers of limestone, while the presence of sand is negligible. Consequently, the production is anticipated to come from the sandstone zones within the formation. These findings provide valuable insights for further exploration and development strategies related to the Abu Roash "G" reservoir.

5. Discussion

The Late Cretaceous Abu Roash "G" reservoirs in the East Alam El-Shawish field, Western Desert, Egypt, have been extensively studied to understand their rock typing and petrophysical characteristics for effective oil development. This study provides valuable insights into reservoir characterization through lithology determination, facies analysis, and petrophysical analysis. When comparing these results with similar studies in the literature [2, 5, 32], several commonalities and distinctions emerge.

The lithology determination of the reservoir was accomplished through the utilization of neutron-density cross plots and M-N cross plots, which provided valuable insights into the composition and characteristics of the lithologies, including sandstone, limestone, and shale. Lithology determination is a crucial step in reservoir

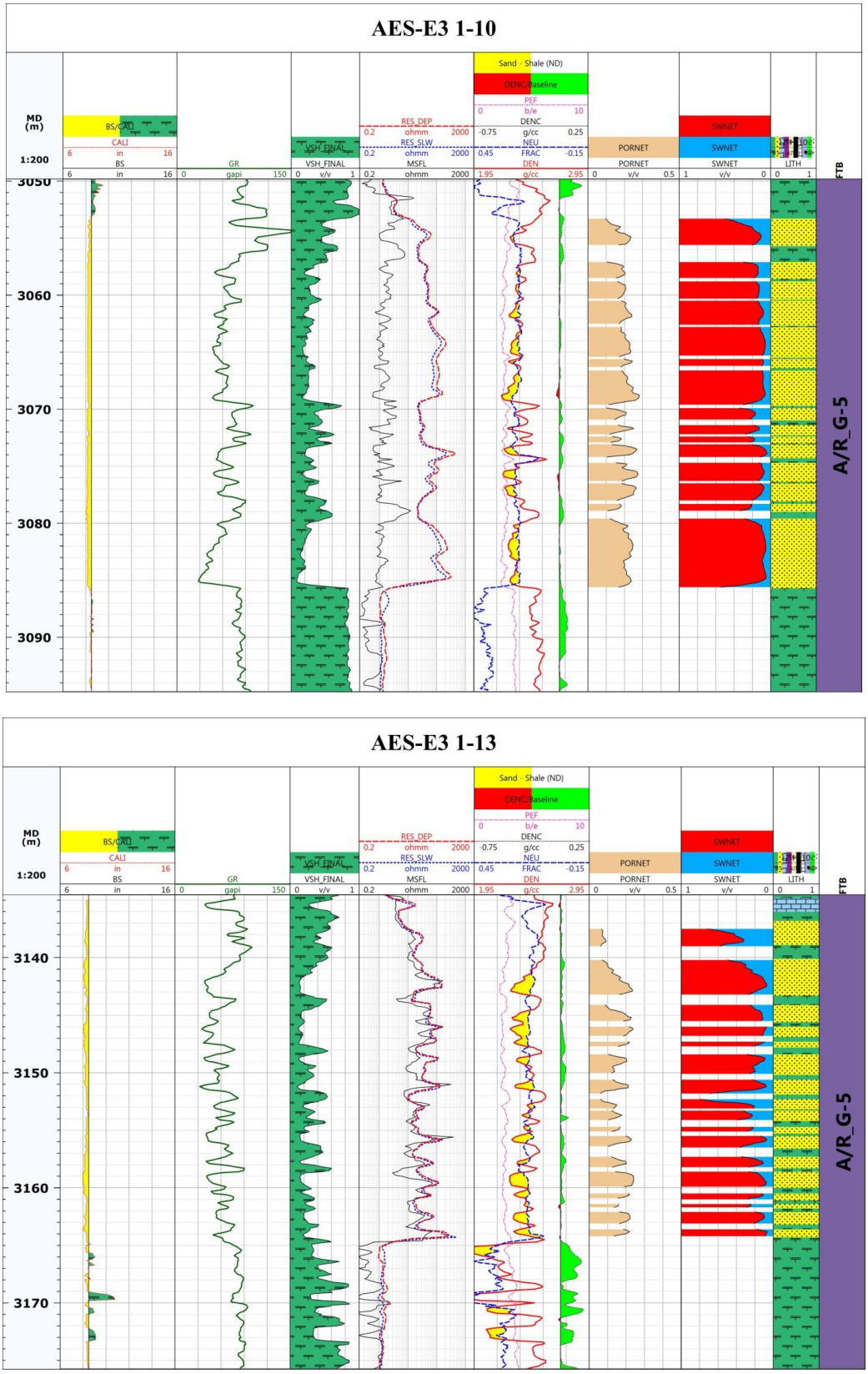

Figure 12: Petrophysical analysis and lithology of Abu Roash"G-5 " reservoir in wells AES-E3 1-10 and AES-E3 1-13.

characterization. Neutron-density cross plots and M-N cross plots have been utilized to determine the lithologies present in the Abu Roash "G" reservoir. Neutron-density cross plots provide insights into the composition of lithologies such as sandstone, limestone, and dolomite. The positions of plotted points relative to lithology lines on the cross plot help identify specific lithologies. The presence of sandstone and calcareous sandstone within the reservoir has been confirmed through this analysis. The influence of gas and shale on the reservoir's characteristics has also been observed. The analysis revealed variations in porosity, emphasizing the heterogeneity of the lithologies within the reservoir. The M-N cross-plot analysis complements the neutron-density cross-plot analysis and provides further insights into lithology determination. By examining the cross plot generated using neutron porosity and micro-resistivity measurements, additional lithological information has been obtained. The results align with those from the neutron-density cross plot, confirming the presence of sandstone and calcareous sandstone lithologies. The influence of shale on neutron porosity values has also been observed in this analysis.

Neutron-density cross-plots are commonly used in geology to assess matrix porosity in carbonate rocks. By plotting bulk density (RHOB) and neutron porosity (NPHI) measurements, lithologies saturated with water, such as sandstone and limestone, can be identified. The analysis of the cross plot for the Abu Roash "G" reservoir revealed the presence of sandstone and calcareous sandstone lithologies based on the positioning of the plotted points relative to the lithology lines. The variation in porosity values (12% to 26%) emphasized the heterogeneity of the lithologies and highlighted the importance of porosity assessment in characterizing the reservoir. The M-N cross-plot analysis, which involved neutron porosity (NPHI) and micro-resistivity (M) measurements, further confirmed the lithological composition of the reservoir, particularly the presence of sandstone and calcareous sandstone. The shale effect, observed in both cross-plot analyses, helped understand the influence of shale on the reservoir's characteristics, contributing to accurate lithology and porosity assessments.

The facies analysis of the Abu Roash "G" reservoir involved the examination of cored intervals in the AES-E3 (1-10) well. Various lithologies were observed, including limestone, sandstone, shale, marls, and different sandstone facies with distinct characteristics. These sandstone facies exhibited different colors, grain sizes, sorting, sedimentary structures, and mineral compositions. The facies analysis identified two facies associations representing different depositional environments—a shallow marine environment and a relatively deeper marine environment. The characterization of these facies associations provided insights into the potential reservoir quality of the lithologies. Facies analysis of the Abu Roash "G" reservoir has been conducted based on the examination of cored intervals in a well. The lithological sequence observed includes various colors and sedimentary features such as vuggy, phosphatic, argillaceous, dolomitic, bioturbated, glauconitic, and carbonaceous matter-bearing lithologies, as well as interbeds of marls and shale. Sandstone facies within this sequence exhibit different characteristics, including grain size variations, silt and clay content, bioturbation, and the presence of minerals such as pyrite and phosphate. The facies analysis has allowed for the identification of distinct lithofacies types and their grouping into two facies associations, providing insights into depositional environments and potential reservoir quality.

The petrophysical analysis of the Abu Roash "G" reservoir involved the assessment of core samples and the classification of reservoir rock types based on their petrophysical attributes. Different reservoir rock types were identified, ranging from cross-bedded sandstone to sandy siltstone. Each rock type exhibited variations in grain density, porosity, permeability, flow zone indicator (FZI), and reservoir quality index (RQI). The analysis indicated that certain rock types, such as cross-bedded sandstone and laminated sandstone, displayed excellent reservoir attributes with high porosity, permeability, and reservoir quality. Petrophysical analysis plays a crucial role in understanding reservoir behavior and characteristics. The petrophysical analysis of the Abu Roash "G" sand reservoir has involved the assessment of core samples and the classification of reservoir rock types based on petrophysical attributes. The analysis has revealed variations in grain density, porosity, permeability, flow zone indicator (FZI), and reservoir quality index (RQI) among the different rock types. Reservoir rock types such as cross-bedded sandstone, laminated sandstone, rippled sandstone, and massive sandstone exhibit high porosity, good permeability, and very good reservoir quality. On the other hand, sandy siltstone and heterolithic alternating sandstone exhibit low porosity, low permeability, and lower reservoir quality. These petrophysical analyses provide valuable insights into the reservoir's potential and the spatial distribution of different lithologies.

While the study provides valuable insights into the Late Cretaceous Abu Roash "G" reservoirs, there are several potential sources of error and uncertainty that should be considered when interpreting their results. Firstly, measurement errors could affect the accuracy of the lithology determination through neutron-density cross plots and M-N cross plots. Variability in instrument calibration or sensitivity could introduce discrepancies in the plotted data, potentially leading to misinterpretations of lithologies. Secondly, sample variations in the core analysis may not fully represent the reservoir's heterogeneity. The limited number of core samples and the localized nature of the sampling can result in uncertainties regarding the broader lithological diversity and distribution within the reservoir [46]. Different intervals in the reservoir might exhibit distinct characteristics that are not fully captured by the analyzed core samples. Additionally, the interpretation of facies from core samples is subject to some degree of subjectivity [47]. The interpretations may vary, affecting the identification of specific lithofacies types and their grouping into facies associations [48-51]. This subjectivity can introduce uncertainties in understanding the depositional environments and potential reservoir quality. Furthermore, while the petrophysical analysis provides valuable information about reservoir rock types, grain density, porosity, and permeability, it is essential to recognize that these attributes can vary spatially within the reservoir. The analysis might not capture the full complexity of heterogeneity, which can impact reservoir behavior and production optimization [52, 53].

6. Conclusions

The Abu Roash "G" Member in AES-E3 (1/10) well, located in the East Alam El Shawish field, was studied petrophysically, resulting in the identification of seven distinct reservoir rock types. These rock types are classified as follows: (RRT1) Cross Bedded Sandstone, (RRT2) Laminated Sandstone, (RRT3) Rippled Sandstone, (RRT4) Massive Sandstone, (RRT5) Silty Sandstone, (RRT6) Heterolithic Alternated Sandstone and Thin Siltstone, and (RRT7) Sandy Siltstone. The reservoir rock types RRT1, RRT2, and RRT3 exhibit very good reservoir quality based on the Reservoir Quality Index (RQI) and the average flow zone indicator. RRT1 samples, characterized by Cross Bedded Sandstone, demonstrate the best reservoir attributes, with a very strong reservoir quality indicated by the average flow zone indicator. RRT2 samples, classified as Laminated Sandstone, show very good porosity and permeability, along with high RQI values, indicating extremely good reservoir quality. Similarly, RRT3 samples, identified as Rippled Sandstone, exhibit very good porosity and very strong permeability values, with the average flow zone indicator also indicating very good reservoir quality.

RRT4, categorized as Massive Sandstone, displays good porosity and permeability values, along with good RQI values. The average flow zone indicator suggests an intermediate reservoir quality for this rock type. RRT5, representing Silty Sandstone, exhibits moderate porosity and permeability, with RQI values indicating moderate reservoir quality. The average flow zone indicator also points to a moderate reservoir quality for RRT5 samples. On the other hand, RRT6, characterized by Heterolithic Alternated Sandstone and Thin Siltstone, demonstrates low permeability and low porosity. Both the RQI values and the average flow zone indicator indicate poor reservoir quality for this rock type. Finally, RRT7, classified as Sandy Siltstone, shows the lowest reservoir quality among the studied rock types, with poor porosity and very low permeability. The RQI values and the average flow zone indicator confirm the very low reservoir quality of RRT7 samples.

Future research and applications in the study of the Abu Roash "G" Member should focus on optimizing reservoir development and recovery strategies based on the identified rock types. This includes fine-tuning drilling and completion techniques tailored to the distinct reservoir qualities of each rock type, as well as investigating the potential for Enhanced Oil Recovery (EOR) methods, especially for rock types with lower reservoir quality. Additionally, the integration of advanced technologies such as machine learning and data analytics into reservoir modeling and decision-making processes can enhance the accuracy of predictions and assist in real-time reservoir management. Further studies should also aim to understand the geological and fluid dynamics interactions among these rock types to improve reservoir performance and maximize hydrocarbon recovery in this complex reservoir.

Conflict of Interest

The authors declare that there is no conflict of interest.

Acknowledgments

We would like to extend our sincere appreciation to the Egyptian General Petroleum Corporation (EGPC) and Petrosannan Petroleum Company for granting us the necessary approvals and permissions to utilize the material for our study. Their cooperation and support have been invaluable in enabling us to conduct our research effectively.

References

[1] Abdel-Fattah MI, Metwalli FI, Mesilhi ESI. Static reservoir modeling of the Bahariya reservoirs for the oilfields development in South Umbarka area, Western Desert, Egypt. J Afr Earth Sci. 2018; 138: 1-13. https://doi.org/10.1016/j.jafrearsci.2017.11.002

[2] Abdelwahhab MA, Raef A. Integrated reservoir and basin modeling in understanding the petroleum system and evaluating prospects: The Cenomanian reservoir, Bahariya Formation, at Falak Field, Shushan Basin, Western Desert, Egypt. J Pet Sci Eng. 2020; 189: 107023. https://doi.org/10.1016/j.petrol.2020.107023

[3] Abdelwahhab MA, Radwan AA, Mahmoud H, Mansour A. Geophysical 3D-static reservoir and basin modeling of a Jurassic estuarine system (JG-Oilfield, Abu Gharadig basin, Egypt). J Asian Earth Sci. 2022; 225: 105067. https://doi.org/10.1016/j.jseaes.2021.105067

[4] Imam TS, Abdel-Fattah MI, Tsuji T, Hamdan HA. Mapping the geological structures in the Ras El Ush field (Gulf of Suez, Egypt), based on seismic interpretation and 3D modeling techniques. J Afr Earth Sci. 2022; 193: 104596. https://doi.org/10.1016/j.jafrearsci.2022.104596

[5] Abdel-Fattah MI, Sen S, Abuzied SM, Abioui M, Radwan AE, Benssaou M. Facies analysis and petrophysical investigation of the Late Miocene Abu Madi sandstones gas reservoirs from offshore Baltim East field (Nile Delta, Egypt). Mar Pet Geol. 2022; 137: 105501. https://doi.org/10.1016/j.marpetgeo.2021.105501

[6] Abdel-Fattah MI, Mahdi AQ, Theyab MA, Pigott JD, Abd-Allah ZM, Radwan AE. Lithofacies classification and sequence stratigraphic description as a guide for the prediction and distribution of carbonate reservoir quality: A case study of the Upper Cretaceous Khasib Formation (East Baghdad oilfield, central Iraq). J Pet Sci Eng. 2022; 209: 109835. https://doi.org/10.1016/j.petrol.2021.109835

[7] Abdelmaksoud A, Amin AT, El-Habaak GH, Ewida HF. Facies and petrophysical modeling of the Upper Bahariya Member in Abu Gharadig oil and gas field, north Western Desert, Egypt. J Afr Earth Sci. 2019; 149: 503-16. https://doi.org/10.1016/j.jafrearsci.2018.09.011

[8] Abuamarah BA, Nabawy BS, Shehata AM, Kassem OMK, Ghrefat H. Integrated geological and petrophysical characterization of oligocene deep marine unconventional poor to tight sandstone gas reservoir. Mar Pet Geol. 2019; 109: 868-85. https://doi.org/10.1016/j.marpetgeo.2019.06.037

[9] Elhossainy MM, Abdelmaksoud A, Ali M, Alrefaee HA. Integrated sedimentological and petrophysical characterization of the Lower Cenomanian clastic Bahariya reservoir in Abu Gharadig Basin, Western Desert, Egypt. J Afr Earth Sci. 2021; 184: 104380. https://doi.org/10.1016/j.jafrearsci.2021.104380

[10] Sarhan MA. Geophysical appraisal for the sandy levels within Abu Roash C and E members in Abu Gharadig Field, Western Desert, Egypt. J Pet Explor Prod Technol. 2021; 11: 1101-22. https://doi.org/10.1007/s13202-021-01107-3

[11] Abdel-Fattah MI, Sarhan MA, Ali AS, Hamdan HA. Structural and petrophysical characteristics of the Turonian "AR/G" reservoirs in heba field (Western Desert, Egypt): Integrated approach for hydrocarbon exploration and development. J Afr Earth Sci. 2023; 207: 105072. https://doi.org/10.1016/j.jafrearsci.2023.105072

[12] Zhu S, Wang X, Qin Y, Jia Y, Zhu X, Zhang J, *et al*. Occurrence and origin of pore-lining chlorite and its effectiveness on preserving porosity in sandstone of the middle Yanchang Formation in the southwest Ordos Basin. Appl Clay Sci. 2017; 148: 25-38. https://doi.org/10.1016/j.clay.2017.08.005

[13] Tobin RC, McClain T, Lieber RB, Ozkan A, Banfield LA, Marchand AME, *et al*. Reservoir quality modeling of tight-gas sands in Wamsutter field: Integration of diagenesis, petroleum systems, and production data. Am Assoc Pet Geol Bull. 2010; 94: 1229-66. https://doi.org/10.1306/04211009140

[14] Worden RH, Armitage PJ, Butcher AR, Churchill JM, Csoma AE, Hollis C, *et al*. Petroleum reservoir quality prediction: overview and contrasting approaches from sandstone and carbonate communities. Geological Society, London: Special Publications; 2018; 435: 1-31. https://doi.org/10.1144/SP435.21

[15] Shehata AA, Sarhan MA, Abdel-Fattah MI, Assal EM. Sequence stratigraphic controls on the gas-reservoirs distribution and characterization along the Messinian Abu Madi incision, Nile Delta Basin. Mar Pet Geol. 2023; 147: 105988. https://doi.org/10.1016/j.marpetgeo.2022.105988

[16] Abdou A. Deep wells in Khalda West: A brief review. 14th EGPC Petroleum Conference, Cairo: 1998.

[17] Amaefule JO, Altunbay M, Tiab D, Kersey DG, Keelan DK. Enhanced reservoir description: using core and log data to identify hydraulic (flow) units and predict permeability in uncored intervals/wells. Annual Technical Conference and Exhibition, Houston, Texas: OnePetro; October 3-6, 1993. https://doi.org/10.2118/26436-MS

[18] Dolson JC, Shann M V, Matbouly SI, Hammouda H, Rashed RM. Egypt in the twenty-first century: petroleum potential in offshore trends. GeoArabia 2001; 6: 211-30. https://doi.org/10.2113/geoarabia0602211

[19] Basheer AA, Metwalli FI, Amin AT, El-Dabaa SA. A new hydrocarbon prospect determination using the seismic interpretation and petrophysical evaluation of Bahariya reservoir in Nader field, north Western Desert, Egypt. J Afr Earth Sci. 2023; 200: 104891. https://doi.org/10.1016/j.jafrearsci.2023.104891

[20] Wasfi SH. Biostratigraphic zonation of the Abu Roash formation in the western desert Egypt. 1973.

[21] Tahoun SS, Deaf AS. Could the conventionally known Abu Roash "G" reservoir (upper Cenomanian) be a promising active hydrocarbon source in the extreme northwestern part of Egypt? Palynofacies, palaeoenvironmental, and organic geochemical answers. Mar Pet Geol. 2016; 76: 231-45. https://doi.org/10.1016/j.marpetgeo.2016.05.025

[22] EGPC (Egyptian General Petroleum Corporation). Western desert, oil and Gas fields, a comprehensive overview. 11th Petroleum Exploration and Production Conference, Cairo: EGPC; 7-10 November 1992.

[23] El Gezeery N, O'connor T. Cretaceous rock units of the western desert, Egypt. 13th Annual Meeting of Geological Society of Egypt, Cairo : Geological Society; 1975, p. 2.

[24] Darwish M, Abdel Hamid M, Fahmy K. Geology and mode of hydrocarbon occurrence in the late cenomanian-early turonian, Abu Sannan area, western desert, Egypt. Earth Sci Ser. 1989; 3: 106-27.

[25] Said R. The geology of Egypt. Rotterdam/Brookfield: AA Balkema;1962.

[26] Fadul MF, El Dawi MG, Abdel-Fattah MI. Seismic interpretation and tectonic regime of Sudanese Rift System: Implications for hydrocarbon exploration in Neem field (Muglad Basin). J Pet Sci Eng. 2020; 191: 107223. https://doi.org/10.1016/j.petrol.2020.107223

[27] Tammam M. Basin modeling of Qarun and west Qarun area and its implication on hydrocarbon generation, western desert, Egypt. Proceedings of the 13th of the Petroleum Conference of Egyptian General Petroleum Corporation, 1996, p. 433–46.

[28] Hussein HM, Abd-Allah AM. Plate tectonics and geological evolution of Egypt. J Afr Earth Sci. 2001; 33: 475-96.

[29] Bakry G, Eid A. Fault/seal paradox in the Abu Gharadig basin. 13th Petroleum Exploration and Production Conference, Cairo: EGPC; 1996, p. 81-96.

[30] El Nady M, Hammad M. Evaluation of cretaceous hydrocarbon source rock in Badr El Din Concession, North Western Desert. J Environ Sci. 2000; 20: 25-51.

[31] Selim ES, Sarhan MA. New stratigraphic hydrocarbon prospects for the subsurface Cretaceous: tertiary succession within Abu Gharadig Basin in the framework of sequence stratigraphic analyses, north Western Desert, Egypt. EuroMediterr J Environ Integr. 2023: 1–8. https://doi.org/10.1007/s41207-023-00403-0

[32] Sarhan MA. Seismic delineation and well logging evaluation for albian Kharita Formation, South West Qarun (SWQ) field, Gindi Basin, Egypt. J Afr Earth Sci. 2019; 158: 103544. https://doi.org/10.1016/j.jafrearsci.2019.103544

[33] Sarhan MA. Possibility of intrusive igneous body beneath the Cretaceous sequence in Abu Gharadig Basin, Egypt: Integration of geophysical data interpretations. Arab J Geosci. 2020; 13: Article number: 445. https://doi.org/10.1007/s12517-020-05436-1

[34] Sharaf L, Ghanem M, Hussein S, El Nady M. Contribution to petroleum source rocks and thermal maturation of Jurassic-Cretaceous sequence, south Matruh, northern Western Desert, Egypt. Sedimentol Egypt. 1999; 7: 71-83.

[35] Wong TF, Baud P. Mechanical compaction of porous sandstone. Oil Gas Sci Tech. 1999; 54: 715-27. https://doi.org/10.2516/ogst:1999061

[36] Shehata AA, Sarhan MA. Seismic interpretation and hydrocarbon assessment of the post-rift Cenomanian Bahariya reservoir, Beni Suef Basin, Egypt. J Pet Explor Prod Technol. 2022; 12: 3243-61. https://doi.org/10.1007/s13202-022-01520-2

[37] Moustafa AR, Saoudi A, Moubasher A, Ibrahim IM, Molokhia H, Schwartz B. Structural setting and tectonic evolution of the Bahariya Depression, Western Desert, Egypt. GeoArabia. 2003; 8: 91-124. https://doi.org/10.2113/geoarabia080191

[38] Shehata AA, El Fawal FM, Ito M, Aboulmagd MA, Brooks HL. Senonian platform-to-slope evolution in the tectonically-influenced Syrian Arc sedimentary belt: Beni Suef Basin, Egypt. J Afr Earth Sci. 2020; 170: 103934. https://doi.org/10.1016/j.jafrearsci.2020.103934

[39] Serra O. Fundamentals of well-log interpretation. New York: Elsevier; 1984.

[40] Abdel-Fattah MI. Petrophysical characteristics of the messinian abu madi formation in the baltim east and north fields, offshore Nile delta, Egypt. J Pet Geol. 2014; 37: 183-95. https://doi.org/10.1111/jpg.12577

[41] Poupon A, Leveaux J. Evaluation of water saturation in shaly formations. Log Anal. 1971; 12: 1-2.

[42] Schlumberger. Log interpretation manual/applications. Vol. 2. Houston: Schlumberger Well Service, Inc.; 1974.

[43] Burke JA, Schmidt AW, Campbell J, Raymond L. The litho-porosity cross plot: a method of determining rock characteristics for computation of log data. Log Anal. 1969; 10: 25-43.

[44] Wilson MJ, Shaldybin MV, Wilson L. Clay mineralogy and unconventional hydrocarbon shale reservoirs in the USA. I. Occurrence and interpretation of mixed-layer R3 ordered illite/smectite. Earth Sci Rev. 2016; 158: 31-50. https://doi.org/10.1016/j.earscirev.2016.04.004

[45] Riazi Z. Application of integrated rock typing and flow units identification methods for an Iranian carbonate reservoir. J Pet Sci Eng. 2018; 160: 483-97. https://doi.org/10.1016/j.petrol.2017.10.025

[46] Shehata AA, Sarhan MA, Abdel-Fattah MI, Mansour S. Geophysical assessment for the oil potentiality of the Abu Roash "G" reservoir in West Beni Suef Basin, Western Desert, Egypt. J Afr Earth Sci. 2023; 199: 104845. https://doi.org/10.1016/j.jafrearsci.2023.104845

[47] Sarhan MA, Ali AS, Abdel-Fattah MI. Geophysical assessment of basement rocks for use as an unconventional reservoir in the Rabeh East oil field, southern Gulf of Suez Basin. EuroMediterr J Environ Integr. 2023; 8: 409-23. https://doi.org/10.1007/s41207-023-00372-4

[48] Worden RH, Morad S. Quartz cementation in oil field sandstones: a review of the key controversies. Quartz Cementation in Sandstones, Wiley; 2000, p. 1–20. https://doi.org/10.1002/9781444304237.ch1

[49] Al-Ramadan K, Morad S, Proust JN, Al-Aasm I. Distribution of diagenetic alterations in siliciclastic shoreface deposits within a sequence stratigraphic framework: evidence from the Upper Jurassic, Boulonnais, NW France. J Sediment Res. 2005; 75: 943-59. https://doi.org/10.2110/jsr.2005.072

[50] Palabiran M, Akbar MNA, Listyaningtyas SN. An analysis of rock typing methods in carbonate rocks for better carbonate reservoir characterization: A case study of Minahaki Carbonate Formation, Banggai Sula Basin, Central Sulawes. In 41th Scientific Annual Meeting of Indonesian Association of Geophysicists (Pit Hagi) Lampung, (Aip Conference Proceedings), 2016

[51] Ewida HF, Sarhan MA. Efficiency of post-stack processing in enhancing seismic data quality: a case study of Southwest Qarun-Field, Gindi Basin, Egypt. EuroMediterr J Environ Integr. 2023: 1-9. https://doi.org/10.1007/s41207-023-00401-2

[52] Zhang X, Lin C-M, Cai Y-F, Qu C-W, Chen Z-Y. Pore-lining chlorite cements in lacustrine-deltaic sandstones from the upper Triassic Yanchang formation, Ordos Basin, China. J Pet Geol. 2012; 35: 273-90. https://doi.org/10.1111/j.1747-5457.2012.00530.x

[53] Zhang K, Guo Y, Bai G, Wang Z, Fan B, Wu J, *et al*. Pore-structure characterization of the Eocene Sha-3 sandstones in the Bohai Bay Basin, China. Energy & Fuels. J Pet Geol. 2012; 35: 1579-91. https://doi.org/10.1111/j.1747-5457.2012.00530.x